



Published in final edited form as:

*Otolaryngol Head Neck Surg.* 2022 November ; 167(5): 860–868. doi:10.1177/01945998221083506.

## RAD51 Inhibitor and Radiation Toxicity in Vestibular Schwannoma

Torin P. Thielhelm, BS<sup>1</sup>, Aida Nourbakhsh, MD, PhD<sup>1</sup>, Scott M. Welford, PhD<sup>2</sup>, Eric A. Mellon, MD PhD<sup>2</sup>, Olena Bracho, BS<sup>1</sup>, Michael E. Ivan, MD MBS<sup>3</sup>, Fred Telischi, MD<sup>1</sup>, Cristina Fernandez-Valle, PhD<sup>4</sup>, Christine T. Dinh, MD<sup>1</sup>

<sup>1</sup>Department of Otolaryngology, University of Miami Miller School of Medicine, Miami, FL

<sup>2</sup>Department of Radiation Oncology, Sylvester Comprehensive Cancer Center, University of Miami Miller School of Medicine, Miami, FL

<sup>3</sup>Department of Neurological Surgery, University of Miami Miller School of Medicine, Miami, FL

<sup>4</sup>Burnett School of Biomedical Sciences, University of Central Florida, College of Medicine, Orlando, FL

### Abstract

**Objective:** Describe the RAD51 (DNA repair) response to radiation-induced DNA damage in patient-derived vestibular schwannoma (VS) cells and investigate the utility of RAD51 inhibitor (RI-1) in enhancing radiation toxicity.

**Study Design:** Basic science, translational

**Setting:** Tertiary academic facility

**Methods:** VS tumors (n=10) were cultured on 96-well plates and 16-well slides, exposed to radiation (0, 6, 12, or 18 Gy), and treated with RI-1 (RAD51 inhibitor; 0, 5, or 10  $\mu$ M). Immunofluorescence was performed at 6 hours for  $\gamma$ -H2AX (DNA damage marker), RAD51 (DNA repair protein), and p21 (cell cycle arrest protein). Viability assays were performed at 96 hours, and capillary western blotting (WB) was utilized to determine RAD51 expression in naïve VS tumors (n=5).

---

**Corresponding Author:** Christine T. Dinh, MD, Associate Professor of Otolaryngology, Otolaryngology, Neurology, Lateral Skull Base Surgery, University of Miami Miller School of Medicine, Address: 1120 NW 14<sup>th</sup> Street, Suite 579, Miami, FL 33136, Phone: (305) 243-1484; Fax: (305) 243-2009, ct Dinh@med.miami.edu.

Author Contributions:

Torin P. Thielhelm: design/conduct/analysis, manuscript drafting/revision, final approval, agree to accountability

Aida Nourbakhsh: design/interpretation, manuscript revision, final approval, agree to accountability

Scott M. Welford: design/interpretation, manuscript revision, final approval, agree to accountability

Eric A. Mellon: design/interpretation, manuscript revision, final approval, agree to accountability

Olena Bracho: design/conduct/analysis, manuscript revision, final approval, agree to accountability

Michael E. Ivan: design/interpretation, manuscript revision, final approval, agree to accountability

Fred Telischi: design/interpretation, manuscript revision, final approval, agree to accountability

Cristina Fernandez-Valle: design/interpretation, manuscript revision, final approval, agree to accountability

Christine T. Dinh: design/conduct/analysis, manuscript drafting/revision, final approval, agree to accountability

Disclosures:

No relevant conflicts of interest.

**Presented:** American Academy of Otolaryngology—Head and Neck Surgery 2021 Annual Meeting, Los Angeles, CA, October 3, 2021

**Results:** VS tumors expressed RAD51. In cultured VS cells, radiation initiated dose-dependent increases in  $\gamma$ -H2AX and p21 expression. VS cells upregulated RAD51 to repair DNA damage following radiation. Addition of RI-1 reduced RAD51 expression in a dose-dependent manner and was associated with increased  $\gamma$ -H2AX levels and decreased viability in a majority of cultured VS tumors.

**Conclusion:** VS may evade radiation injury by entering cell cycle arrest and upregulating RAD51-dependent repair of radiation-induced double-stranded breaks in DNA. Although there was variability in responses amongst individual primary VS cells, RAD51 inhibition with RI-1 reduce RAD51-dependent DNA repair to enhance radiation toxicity in VS cells. Further investigations are warranted to understand the mechanisms of radiation resistance in VS and determine whether RI-1 is an effective radiosensitizer in patients with VS.

### Keywords

vestibular schwannoma; VS; radiation; resistance; H2AX; p21; RAD51; cell cycle arrest; RAD51 inhibitor

---

### Introduction:

Vestibular schwannomas (VS) are benign tumors of Schwann cells in the cochleovestibular nerve and are the most common tumors of the cerebellopontine angle (CPA). VS account for 8–10% of all intracranial tumors with a prevalence of 1 in every 2000 adults<sup>1–3</sup>. Because of their position at the CPA and internal auditory canal, VS can result in vertigo or imbalance, hearing loss, and tinnitus. Larger tumors can grow into the brainstem and cerebellum, resulting in serious complications such as hydrocephalus, brain herniation, and death<sup>4,5</sup>. Management options, which vary based on symptoms and tumor size, include observation, stereotactic radiosurgery (SRS), and surgery<sup>6,7</sup>.

Approximately 25% of VS are treated with SRS as the initial treatment choice<sup>8</sup>. SRS is a radiation therapy that allows for specific targeting of radiation doses to a defined anatomical area<sup>9</sup>. This is important in the treatment of VS, as key structures like the cochlea and brainstem are within close proximity to the target area. Notably, the progression-free survival (PFS) rate after SRS is approximately 84–94%<sup>10–15</sup>. However, a subset of VS do not respond to SRS and continue to grow<sup>13,14</sup>. The exact mechanisms behind this radiation resistance are poorly understood<sup>12,16</sup>.

Ionizing radiation (IR) creates DNA damage, which exists as both single and double-stranded breaks (DSBs). DSBs activate the ataxia-telangiectasia mutated (ATM) protein, which phosphorylates serine-139 on the minor histone H2A variant and forms  $\gamma$ -H2AX<sup>17</sup>.  $\gamma$ -H2AX is therefore a marker of DNA DSBs<sup>18</sup>. Several DNA repair enzymes attempt to repair DNA damage through various methods. RAD51 is a DNA repair enzyme that serves as the main protein involved in a repair mechanism called homologous recombination (HR). RI-1 is a small molecule inhibitor of RAD51 that has been studied as a radiosensitizer in glioma stem cells<sup>19,20</sup>. RI-1 irreversibly inhibits HR by covalently binding to RAD51, thus interfering with interactions between individual RAD51 subunits and between RAD51 and its cofactor, adenosine triphosphate (ATP)<sup>19</sup>.

In a previous *in vitro* investigation, we demonstrated that some VS display radiation resistance through upregulation of p21, allowing for a robust cell cycle arrest response to repair DNA damage. We found that a radiation dose of 18 Gray (Gy) resulted in the formation of  $\gamma$ -H2AX and upregulation of RAD51, reflecting the presence of DNA DSBs and DNA repair enzyme activity, respectively<sup>21</sup>. We therefore sought to investigate whether exposure of irradiated VS cells to the RAD51 inhibitor RI-1 could block RAD51-associated DNA damage repair and thereby increase the sensitivity of VS to IR. We performed cell viability assays and immunofluorescent staining for  $\gamma$ -H2AX, RAD51, and p21 in irradiated VS cells to explore the effects of RI-1 on DNA damage, DNA repair, and cell cycle arrest at various radiation dosages.

## Methods:

### Tumor Harvesting

Ten patients with VS were consented for tumor banking through a University of Miami Institutional Review Board-approved protocol (#20150637). Tumors were surgically resected at Jackson Memorial Hospital/University of Miami and stored in chilled Dulbecco's Modified Eagle Medium (DMEM; Gibco). Tumors were then enzymatically dissociated and cultured in T75 flasks pre-coated with 25  $\mu$ g/mL of laminin (ThermoFisher Scientific) and 0.01% poly-L-ornithine (PLO; Sigma-Aldrich) as previously described<sup>21</sup>.

### Retrospective Chart Review

Retrospective chart review was performed for the ten VS patients. The following information was obtained: (1) age, (2) gender, (3) tumor volume (cm<sup>3</sup>), (4) extent of tumor resection, and (5) hearing status (Table 1). Magnetic resonance imaging (MRI) with axial T1 sequences with contrast were processed using MIM software (MIM Software, Inc.) to measure tumor volume. Patient hearing status was classified using the American Academy of Otolaryngology Head and Neck Surgery (AAO-HNS) Hearing Classification Scale<sup>22</sup>.

### Radiation Delivery

Primary human VS cells were irradiated at room temperature with a radiation dose of 0, 6, 12, or 18 Gy delivered by an RS 2000 biological cabinet X-Irradiator (Rad Source Technologies). Radiation was delivered at 1.85 Gy/min at 160 kV and 25.0 mA.

### Cell Viability Assays

Primary human VS cells were plated at 10,000 cells per well on 96-well plates precoated with laminin (25  $\mu$ g/mL) and 0.01% PLO (n=6 per condition). VS cells were cultured in Schwann cell media (Sciencell) at 37 degrees Celsius with 5% CO<sub>2</sub>. After 24 hours *in vitro*, cells were treated with 0, 5, or 10  $\mu$ M of RI-1 (Sigma Aldrich) in maintenance media (DMEM, 10% fetal bovine serum, and 1% penicillin-streptomycin). After another 24 hours *in vitro*, cells were irradiated with 0, 6, 12, or 18 Gy. Cell viability assays (CellTiter-Glo, Promega) were performed at 96 hours after radiation exposure, following the manufacturer's established protocol. Viability was measured with a Glomax luminometer (Promega). Mean fold change (MFC) in cell viability was calculated relative to the 0 Gy condition for each condition.

### Immunofluorescence (IF)

Primary human VS cells were cultured in Schwann cell media at 10,000 cells per well on 16-well culture slides precoated with laminin (25 µg/mL) and 0.01% PLO at 5% CO<sub>2</sub> and 37 degrees Celsius. After 24 hours *in vitro*, cells were treated with 0 µM, 5 µM, or 10 µM of RI-1 in maintenance media. After another 24 hours *in vitro*, cells were exposed to 0, 6, 12, or 18 Gy of IR. Six hours after irradiation, cells were fixed with 4% paraformaldehyde, permeabilized and blocked with 5% donkey serum (Sigma) and 1% Triton X-100 in phosphate buffered saline (PBS) for 2 hours at room temperature. Incubation with primary antibodies was performed overnight at 4 degrees Celsius. The primary antibodies were anti-H2AX (1:200) (GT231, Invitrogen), anti-RAD51 (1:1,000) (ab63801, Abcam), and anti-p21 (1:100) (MA5-14949, ThermoFisher Scientific). Slides were then washed with PBS and incubated with fluorophore-conjugated secondary antibodies (donkey anti-rabbit-Alexa 594, ThermoFisher Scientific, 1:200; donkey anti-mouse-Alexa 488, ThermoFisher Scientific, 1:200). Slides were washed with PBS, stained with 300 nM 4',6-diamidino-2-phenylindole (DAPI; ab104139, Abcam) for 10 minutes at room temperature, and cover-slipped with anti-fade mounting medium (Sigma). Images were obtained with a Leica SP5 inverted confocal microscope and a 40X oil immersion lens. For  $\gamma$ -H2AX and RAD51 expression, nuclear foci were counted per cell (n=6 cells per condition). For p21 expression, the percentage of cells expressing p21 staining was measured (n=6 per condition).

### Capillary Western Blotting (WB)

Protein samples from naïve tumor chunks were available for five of the ten VS studied. Tumor chunks were processed with radioimmunoprecipitation assay buffer and sonicated (Misonix). Protein was isolated and bicinchoninic acid protein assays were performed to obtain protein concentration. Samples were diluted to 400 ng/µL. Automated capillary western blotting using 1.2 µg protein/well and chemiluminescence was performed according to manufacturer's protocol (Jess Simple Western; ProteinSimple). Primary antibodies were anti-RAD51 (1:50) (ab63801, Abcam) and anti-GAPDH (1:150) (#2118, Cell Signaling).

### Statistical Analysis

Cell viability was analyzed using two-way analysis of variance and Tukey-Kramer post-hoc testing. The number of nuclear foci for  $\gamma$ -H2AX and RAD51 were analyzed using 95% confidence intervals (95%CI). Fisher's Exact test was utilized to analyze p21 nuclear expression. Significance was set at *p*-value less than 0.05. Bonferroni correction was applied when analyzing viability for individual VS.

## Results:

### Clinical Characteristics of Patients with Vestibular Schwannoma (VS)

Ten patients with sporadic VS underwent microsurgical resection for VS and were included in the study (Table 1). Of the 10 patients, four were female and six were male. The mean age at surgery was 46.5 years old (range: 28–72 years old). Mean tumor volume was 8.18 cm<sup>3</sup> (range: 0.55–18.34 cm<sup>3</sup>). Seven of the tumors were right-sided while three of the tumors were left-sided. Axial T1-weighted magnetic resonance imaging (MRI) studies with

gadolinium were reviewed for the ten patients (Figure 1). Both VSA73 and VSA78 were revision surgeries for tumor progression after initial resection. Gross total resection was achieved in five of ten patients, near total resection was achieved in three patients, and subtotal resection was achieved in two patients. Two of ten patients had serviceable hearing (AAO-HNS Class A or B) and the remaining eight patients had non-serviceable hearing (AAO-HNS Class C or D).

### Cell Viability by Radiation, RI-1, and Individual VS

Primary human VS cells were treated with 0, 5, or 10  $\mu\text{M}$  RI-1, irradiated with 0, 6, 12, or 18 Gy, and analyzed for cell viability 96 hours after irradiation. At 0, 5, and 10  $\mu\text{M}$  RI-1, radiation caused dose-dependent decreases in the viability of primary VS cells, when compared to the 0 Gy condition ( $p < 0.001$ ; Figure 2). At 0 Gy, the addition of RI-1 at 5 or 10  $\mu\text{M}$  RI-1 did not significantly affect cell viability ( $p = 0.9859$  and  $p = 0.8385$ , respectively). At 6 Gy, 10  $\mu\text{M}$  RI-1 caused a significant reduction in viability when compared to 0  $\mu\text{M}$  RI-1 ( $p < 0.0001$ ), but 5  $\mu\text{M}$  RI-1 did not ( $p = 0.1039$ ). However, both 5 and 10  $\mu\text{M}$  RI-1 caused significant reductions in viability at 12 Gy ( $p = 0.0007$  and  $p < 0.0001$ , respectively) and 18 Gy ( $p < 0.0001$  and  $p < 0.0001$ , respectively), when compared to the 0  $\mu\text{M}$  RI-1 condition.

When analyzed by individual VS, MFC in viability varied significantly amongst irradiated tumor cells (Figure 3). In the 0  $\mu\text{M}$  RI-1 condition, two tumors (VSA62 and VSA73) were resistant to radiation and did not demonstrate viability losses even at the 18 Gy condition; however, treatment with RI-1 at 5 and 10  $\mu\text{M}$  initiated dose-dependent decreases in viability with the greatest decrease occurring at 18 Gy and 10  $\mu\text{M}$  RI-1 for both VSA62 ( $p < 0.0001$ ) and VSA73 ( $p < 0.0001$ ). Among all the VS, the greatest loss in viability was elicited at 18 Gy of radiation and 10  $\mu\text{M}$  RI-1 in VSA73 (i.e.  $> 60\%$  reduction when compared to 0 Gy). Although RI-1 (5 and 10  $\mu\text{M}$ ) enhanced radiation toxicity in most VS, RI-1 was less effective at reducing viability at 6, 12, and 18 Gy radiation dosages with VSA60 and VSA69, suggesting that RAD51 may not be a primary mode of DNA repair in VSA60 and VSA69.

### Immunofluorescence

Immunofluorescent staining for  $\gamma\text{-H2AX}$  and RAD51 was performed on primary human VS cells. At 0, 5, and 10  $\mu\text{M}$  RI-1, radiation induced dose-dependent increases in the number of  $\gamma\text{-H2AX}$  and RAD51 nuclear foci per cell (Figure 4A and 4B, respectively). At 6, 12, and 18 Gy, RI-1 at 10  $\mu\text{M}$  induced the highest numbers of  $\gamma\text{-H2AX}$  and RAD51 nuclear foci per cell, when compared to 0 and 5  $\mu\text{M}$  RI-1 conditions. Confocal images (40X) of  $\gamma\text{-H2AX}$  and RAD51 from a representative VS with and without 10  $\mu\text{M}$  RI-1 are provided in Figure 5.

Immunofluorescent staining was also performed for the cell cycle arrest protein p21. Regardless of the RI-1 dosage (0, 5, and 10  $\mu\text{M}$ ), the percentage of cells expressing nuclear p21 increased progressively with higher radiation dosages ( $p < 0.0001$  at 6, 12, and 18 Gy), when compared to the 0 Gy condition (Figure 6). Notably, there were no significant differences between p21 nuclear expression between the RI-1 dosage groups at 0 Gy ( $p = 0.9102$ ), 6 Gy ( $p = 0.8946$ ), 12 Gy ( $p = 1.000$ ), and 18 Gy ( $p = 0.9356$ ). Representative

confocal images demonstrate p21 expression from one VS (VSA56) at 0  $\mu$ M RI-1 (Figure 7).

### **RAD51 Protein Expression**

To investigate RAD51 expression in VS from individual tumors, we performed automated capillary WB on protein extracted from surgically resected VS tumor chunks. Adequate protein was available from five of the ten VS tumors. Capillary WB for RAD51 protein revealed variable expression of RAD51 between individual tumors (Figure 8). Variability in baseline levels of RAD51 in VS may explain the heterogeneity in response of VS to radiation and treatment with RI-1. In particular, VSA60 and VSA69 tumors had less RAD51 expression overall (Figure 8) and did not have profound shifts in viability when RAD51 inhibitor RI-1 was used in conjunction with radiation (Figure 3).

### **Discussion:**

The exact mechanisms of radiation resistance of VS in patients are largely unknown but are likely related to several factors. These factors may include: (1) insufficient radiation dosages to initiate cell death, (2) efficient DNA repair systems, (3) tumor hypoxia preventing generation of radiation-induced reactive oxygen species, (4) altered expression of tumor suppressor and proto-oncogenes, (5) aberrant expression of cell cycle checkpoint proteins, (6) cumulative effects of the loss of function of the NF2-merlin tumor suppressor on cell proliferation, and (7) prolonged cell cycle arrest for DNA repair<sup>12,16,23–26</sup>. In our previous study, we showed that radioresistant VS cells mount a strong p21 response after radiation exposure (18 Gy), which can direct cells into cell cycle arrest and allow time for RAD51-associated repair of DNA damage<sup>21</sup>.

In this study, we tested 0, 6, 12, and 18 Gy of radiation on primary VS cells from 10 tumors and found that radiation initiated dose-dependent increases in DNA DSBs, cell cycle arrest protein p21, and RAD51-associated DNA repair. We also demonstrated that radiation led to dose-dependent decreases in viability overall and in a majority of tumors, with the exception of VSA62 and VSA73. Pre-treatment with RI-1 enhanced radiation-induced losses in viability by blocking RAD51 activation and increasing DNA injury. More importantly, RI-1 caused reductions in viability of VSA62 and VSA73 cells, which were originally resistant to radiation injury at 6, 12, and 18 Gy of radiation.

In two VS (VSA60 and VSA69), pre-treatment with RI-1 did not significantly enhance radiation toxicity. We showed that individual tumors have variable expression levels of RAD51. VSA60 and VSA69 may have responded poorly to RI-1 because they express less RAD51 at baseline. RI-1 also did not affect p21 expression in irradiated VS cells. These results were expected, as p21 acts upstream of RAD51 in the DNA damage response pathway, while RI-1 acts as an irreversible inhibitor at the level of RAD51 protein<sup>27,28</sup>.

Our results indicate that RAD51 inhibitor RI-1 can radiosensitize a majority of VS by limiting the RAD51-associated DNA repair response. The beneficial effects of RI-1 were observed at 6, 12, and 18 Gy of radiation. Because the number of  $\gamma$ -H2AX and RAD51 nuclear foci were highest at 18 Gy, the greatest reductions in viability occurred in the 18

Gy and 10  $\mu\text{M}$  RI-1 condition. It is important to note that the viability of cells is equivalent between 18 Gy (0  $\mu\text{M}$  RI-1), 12 Gy (5  $\mu\text{M}$  RI-1), and 6 Gy (10  $\mu\text{M}$  RI-1) conditions, suggesting that RI-1 could reduce the amount of radiation necessary to achieve equivalent effects of tumor control. Reducing radiation has several potential benefits, including limiting cochlear toxicity, decreasing facial palsy rates, and reducing the risk of radiation necrosis of the brainstem.

When treating VS with SRS, the goal is to maximize tumor control while minimizing toxicity to essential anatomical structures like the facial nerve, the trigeminal nerve, and the cochlea. Although retrospective investigations have shown that single fraction radiation with GammaKnife SRS (marginal tumor dose of ~11–13 Gy) are associated with tumor control rates of 84–94% in VS<sup>12–15</sup>, facial nerve palsy occurs in approximately ~1% of patients and progression to unserviceable hearing occurs in roughly 75% at 10 years<sup>10,29–33</sup>. Thus, introduction of radiosensitizers, such as RI-1, may improve tumor control rates and/or permit lower dosages of radiation with equivalent tumor control and less toxicity to adjacent neurovascular structures.

Several studies have linked radiation resistance in cancer to the presence of tumor stem cells<sup>34–37</sup>. King et al. showed that two patient-derived glioblastoma stem cell (GSC) lines expressed high levels of RAD51 and rely on RAD51-dependent DNA repair after radiation injury<sup>19</sup>. They also showed that RAD51 inhibitors RI-1 and B02 blocked RAD51 foci formation, reduced repair of DNA DSBs, and improved sensitivity to radiation. In another study, Balbous et al. analyzed the expression of RAD51 following IR in 10 patient-derived GSC lines. They found radiation resistance in GSC lines was associated with higher RAD51 expression after radiation, and RI-1 can help overcome radiation resistance in these cells by reducing DNA repair and inducing apoptosis of cells<sup>20</sup>. Our findings associated with RI-1 are consistent with the aforementioned studies. In our investigation, we demonstrated that VS express RAD51 proteins, and RI-1 can improve radiation sensitivity of patient-derived VS cells, particularly in those expressing higher levels of RAD51.

RI-1 was also tested in an animal model of gliomas. In this study, King et al. implanted U87-MG cells into the flank of BALB/c nude mice. They administered RI-1 (100  $\mu\text{L}$  of 20  $\mu\text{M}$ ) or vehicle via intratumoral injection in three cycles over 5 days. Three hours after each injection, 5 Gy of radiation was delivered to the flank, for a total of 15 Gy. Concurrent treatment with radiation and RI-1 resulted in lower tumor growth rates than vehicle-only, RI-1 only, and radiation-only conditions<sup>19</sup>. In another study involving cervical cancer cells, Chen et al. showed that RI-1 sensitized cancer cells to concurrent chemoradiation with cisplatin and suppressed cell proliferation. RI-1 also suppressed the growth of cervical cancer xenografts<sup>38</sup>. Our study demonstrated that RI-1 at 5 and 10  $\mu\text{M}$  concentrations can reduce viability of irradiated VS cells. Future directions could involve the application of these findings to xenograft models of VS<sup>39</sup>.

One advantage of our study is the use of ten different patient-derived VS cells. Although we evaluated the effects of radiation and RI-1 on viability, DNA damage, and DNA repair mechanisms, we only evaluated one DNA repair mechanism (i.e. RAD51), single fraction radiation, and early time points after irradiation. In addition, our *in vitro* study

design does not reflect the tumor microenvironment of VS, where tumor vasculature and hypoxia play an important role in radiation response. In addition, the proliferation rates can vary among the different sub-populations of VS cells within a single tumor, and radiation may be less effective in some sub-populations than others. *In vivo* models have the benefit of evaluating functional outcomes related to toxicity of normal tissues (e.g. hearing loss) from combination radiation and RAD51 inhibition. Future studies should focus on additional DNA repair mechanisms, different radiation protocols, other radiosensitizers, and effectiveness in animal models.

## Conclusion:

Radiation induced dose-dependent reductions in cell viability in a majority of patient-derived VS. Small molecule inhibitor RI-1 can block RAD51 activation, increase DNA damage, and initiate further losses in viability, especially in radiation-resistant VS cells. The findings of this study support further investigation into the mechanisms of radiation resistance in VS to identify new therapeutic targets and determine the effectiveness of other novel radiosensitizers to overcome radiation resistance in VS.

## Funding:

This study was in part funded in part by the Sylvester Comprehensive Cancer Center NIH/NCI K-supplement Grant (CTD), NIH/NIDCD K08DC017508 (CTD), and the NIH/NIDCD R01DC017264-01 (CFV/XZL).

## References

1. Stangerup SE, Caye-Thomasen P, Tos M, Thomsen J. The natural history of vestibular schwannoma. *Otol Neurotol*. 2006;27(4):547–552. [PubMed: 16791048]
2. Evans DG, Moran A, King A, Saeed S, Gurusinge N, Ramsden R. Incidence of vestibular schwannoma and neurofibromatosis 2 in the North West of England over a 10-year period: higher incidence than previously thought. *Otol Neurotol*. 2005;26(1):93–97. [PubMed: 15699726]
3. Marinelli JP, Grossardt BR, Lohse CM, Carlson ML. Prevalence of Sporadic Vestibular Schwannoma: Reconciling Temporal Bone, Radiologic, and Population-based Studies. *Otol Neurotol*. 2019;40(3):384–390. [PubMed: 30688755]
4. Vellin JF, Bozorg Grayeli A, Kalamarides M, Fond C, Bouccara D, Sterkers O. Intratumoral and brainstem hemorrhage in a patient with vestibular schwannoma and oral anticoagulant therapy. *Otol Neurotol*. 2006;27(2):209–212. [PubMed: 16436991]
5. Carlson ML, Tombers NM, Driscoll CLW, et al. Clinically significant intratumoral hemorrhage in patients with vestibular schwannoma. *Laryngoscope*. 2017;127(6):1420–1426. [PubMed: 27515152]
6. Marinelli JP, Lohse CM, Carlson ML. Incidence of Vestibular Schwannoma over the Past Half-Century: A Population-Based Study of Olmsted County, Minnesota. *Otolaryngol Head Neck Surg*. 2018;159(4):717–723. [PubMed: 29712512]
7. Leon J, Trifiletti DM, Waddle MR, et al. Trends in the initial management of vestibular schwannoma in the United States. *J Clin Neurosci*. 2019;68:174–178. [PubMed: 31324471]
8. Carlson ML, Habermann EB, Wagie AE, et al. The Changing Landscape of Vestibular Schwannoma Management in the United States--A Shift Toward Conservatism. *Otolaryngol Head Neck Surg*. 2015;153(3):440–446. [PubMed: 26129740]
9. Jacob JT, Pollock BE, Carlson ML, Driscoll CL, Link MJ. Stereotactic radiosurgery in the management of vestibular schwannoma and glomus jugulare: indications, techniques, and results. *Otolaryngol Clin North Am*. 2015;48(3):515–526. [PubMed: 25873444]



10. Watanabe S, Yamamoto M, Kawabe T, et al. Stereotactic radiosurgery for vestibular schwannomas: average 10-year follow-up results focusing on long-term hearing preservation. *J Neurosurg.* 2016;125(Suppl 1):64–72. [PubMed: 27903183]
11. Murphy ES, Barnett GH, Vogelbaum MA, et al. Long-term outcomes of Gamma Knife radiosurgery in patients with vestibular schwannomas. *J Neurosurg.* 2011;114(2):432–440. [PubMed: 20095786]
12. Thielhelm TP, Goncalves S, Welford SM, et al. Understanding the Radiobiology of Vestibular Schwannomas to Overcome Radiation Resistance. *Cancers (Basel).* 2021;13:4575. [PubMed: 34572805]
13. Johnson S, Kano H, Faramand A, et al. Long term results of primary radiosurgery for vestibular schwannomas. *J Neurooncol.* 2019;145(2):247–255. [PubMed: 31535315]
14. Smith DR, Saadatmand HJ, Wu CC, et al. Treatment Outcomes and Dose Rate Effects Following Gamma Knife Stereotactic Radiosurgery for Vestibular Schwannomas. *Neurosurgery.* 2019;85(6):E1084–E1094. [PubMed: 31270543]
15. Kaylie DM, Horgan MJ, Delashaw JB, McMenomey SO. A meta-analysis comparing outcomes of microsurgery and gamma knife radiosurgery. *Laryngoscope.* 2000;110(11):1850–1856. [PubMed: 11081598]
16. Dougherty MC, Shibata SB, Hansen MR. The biological underpinnings of radiation therapy for vestibular schwannomas: Review of the literature. *Laryngoscope Investig Otolaryngol.* 2021;6(3):458–468.
17. Shiloh Y, Ziv Y. The ATM protein kinase: regulating the cellular response to genotoxic stress, and more. *Nat Rev Mol Cell Biol.* 2013;14(4):197–210.
18. Mah LJ, El-Osta A, Karagiannis TC. gammaH2AX: a sensitive molecular marker of DNA damage and repair. *Leukemia.* 2010;24(4):679–686. [PubMed: 20130602]
19. King HO, Brend T, Payne HL, et al. RAD51 Is a Selective DNA Repair Target to Radiosensitize Glioma Stem Cells. *Stem Cell Reports.* 2017;8(1):125–139. [PubMed: 28076755]
20. Balbous A, Cortes U, Guilloteau K, et al. A radiosensitizing effect of RAD51 inhibition in glioblastoma stem-like cells. *BMC Cancer.* 2016;16:604. [PubMed: 27495836]
21. Thielhelm TP, Goncalves S, Welford S, et al. Primary Vestibular Schwannoma Cells Activate p21 and RAD51-Associated DNA Repair Following Radiation-Induced DNA Damage. *Otol Neurotol.* 2021;42(10):e1600–e1608. [PubMed: 34420024]
22. Committee on Hearing and Equilibrium guidelines for the evaluation of hearing preservation in acoustic neuroma (vestibular schwannoma). American Academy of Otolaryngology-Head and Neck Surgery Foundation, INC. *Otolaryngol Head Neck Surg.* 1995;113(3):179–180. [PubMed: 7675475]
23. Langenhuisen P, Sebregts SHP, Zinger S, Leenstra S, Verheul JB, de With PHN. Prediction of transient tumor enlargement using MRI tumor texture after radiosurgery on vestibular schwannoma. *Med Phys.* 2020;47(4):1692–1701. [PubMed: 31975523]
24. Gugel I, Ebner FH, Grimm F, et al. Contribution of mTOR and PTEN to Radioresistance in Sporadic and NF2-Associated Vestibular Schwannomas: A Microarray and Pathway Analysis. *Cancers (Basel).* 2020;12(1).
25. Yeung AH, Sughrue ME, Kane AJ, Tihan T, Cheung SW, Parsa AT. Radiobiology of vestibular schwannomas: mechanisms of radioresistance and potential targets for therapeutic sensitization. *Neurosurg Focus.* 2009;27(6):E2.
26. Gross MW, Kraus A, Nashwan K, Mennel HD, Engenhardt-Cabillic R, Schlegel J. Expression of p53 and p21 in primary glioblastomas. *Strahlenther Onkol.* 2005;181(3):164–171. [PubMed: 15756520]
27. Abbas T, Dutta A. p21 in cancer: intricate networks and multiple activities. *Nat Rev Cancer.* 2009;9(6):400–414. [PubMed: 19440234]
28. Karimian A, Ahmadi Y, Yousefi B. Multiple functions of p21 in cell cycle, apoptosis and transcriptional regulation after DNA damage. *DNA Repair (Amst).* 2016;42:63–71. [PubMed: 27156098]
29. Yang I, Sughrue ME, Han SJ, et al. Facial nerve preservation after vestibular schwannoma Gamma Knife radiosurgery. *J Neurooncol.* 2009;93(1):41–48. [PubMed: 19430881]

30. Hasegawa T, Kida Y, Kobayashi T, Yoshimoto M, Mori Y, Yoshida J. Long-term outcomes in patients with vestibular schwannomas treated using gamma knife surgery: 10-year follow up. *J Neurosurg.* 2005;102(1):10–16. [PubMed: 15658090]
31. Carlson ML, Jacob JT, Pollock BE, et al. Long-term hearing outcomes following stereotactic radiosurgery for vestibular schwannoma: patterns of hearing loss and variables influencing audiometric decline. *J Neurosurg.* 2013;118(3):579–587. [PubMed: 23101446]
32. Lunsford LD, Niranjan A, Flickinger JC, Maitz A, Kondziolka D. Radiosurgery of vestibular schwannomas: summary of experience in 829 cases. *J Neurosurg.* 2005;102 Suppl:195–199. [PubMed: 15662809]
33. Hasegawa T, Fujitani S, Katsumata S, Kida Y, Yoshimoto M, Koike J. Stereotactic radiosurgery for vestibular schwannomas: analysis of 317 patients followed more than 5 years. *Neurosurgery.* 2005;57(2):257–265; discussion 257–265. [PubMed: 16094154]
34. Lamb R, Ozsvari B, Bonuccelli G, et al. Dissecting tumor metabolic heterogeneity: Telomerase and large cell size metabolically define a sub-population of stem-like, mitochondrial-rich, cancer cells. *Oncotarget.* 2015;6(26):21892–21905. [PubMed: 26323205]
35. Schulz A, Meyer F, Dubrovska A, Borgmann K. Cancer Stem Cells and Radioresistance: DNA Repair and Beyond. *Cancers (Basel).* 2019;11(6).
36. Arnold CR, Mangesius J, Skvortsova II, Ganswindt U. The Role of Cancer Stem Cells in Radiation Resistance. *Front Oncol.* 2020;10:164. [PubMed: 32154167]
37. Rich JN. Cancer stem cells in radiation resistance. *Cancer Res.* 2007;67(19):8980–8984. [PubMed: 17908997]
38. Chen Q, Cai D, Li M, Wu X. The homologous recombination protein RAD51 is a promising therapeutic target for cervical carcinoma. *Oncol Rep.* 2017;38(2):767–774. [PubMed: 28627709]
39. Dinh CT, Bracho O, Mei C, et al. A Xenograft Model of Vestibular Schwannoma and Hearing Loss. *Otol Neurotol.* 2018;39(5):e362–e369. [PubMed: 29557843]

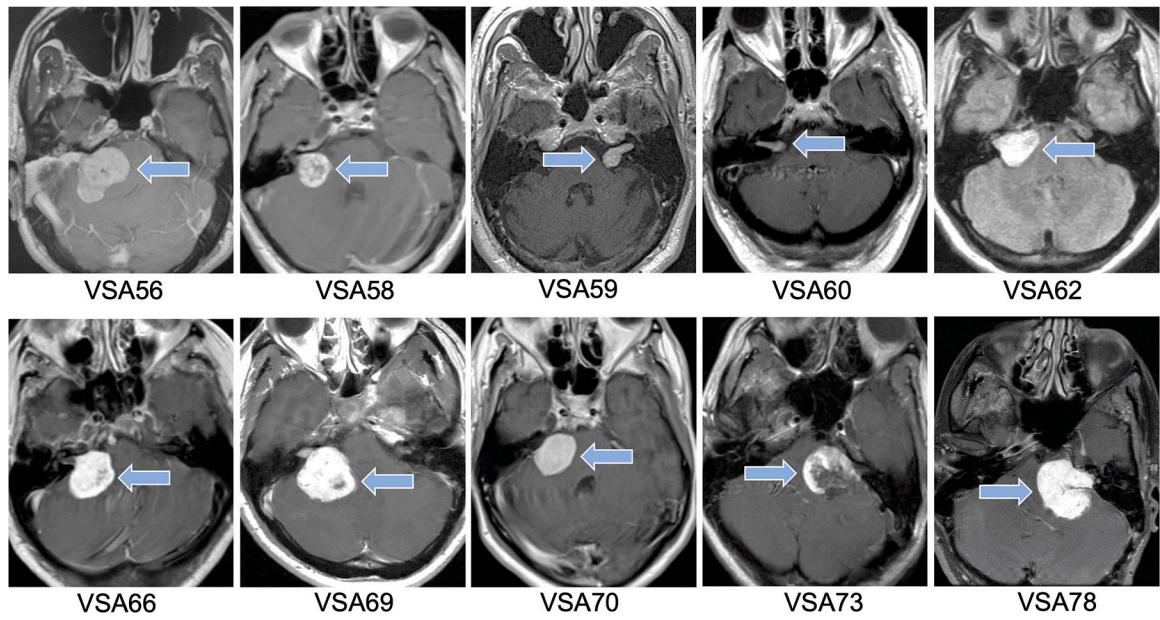
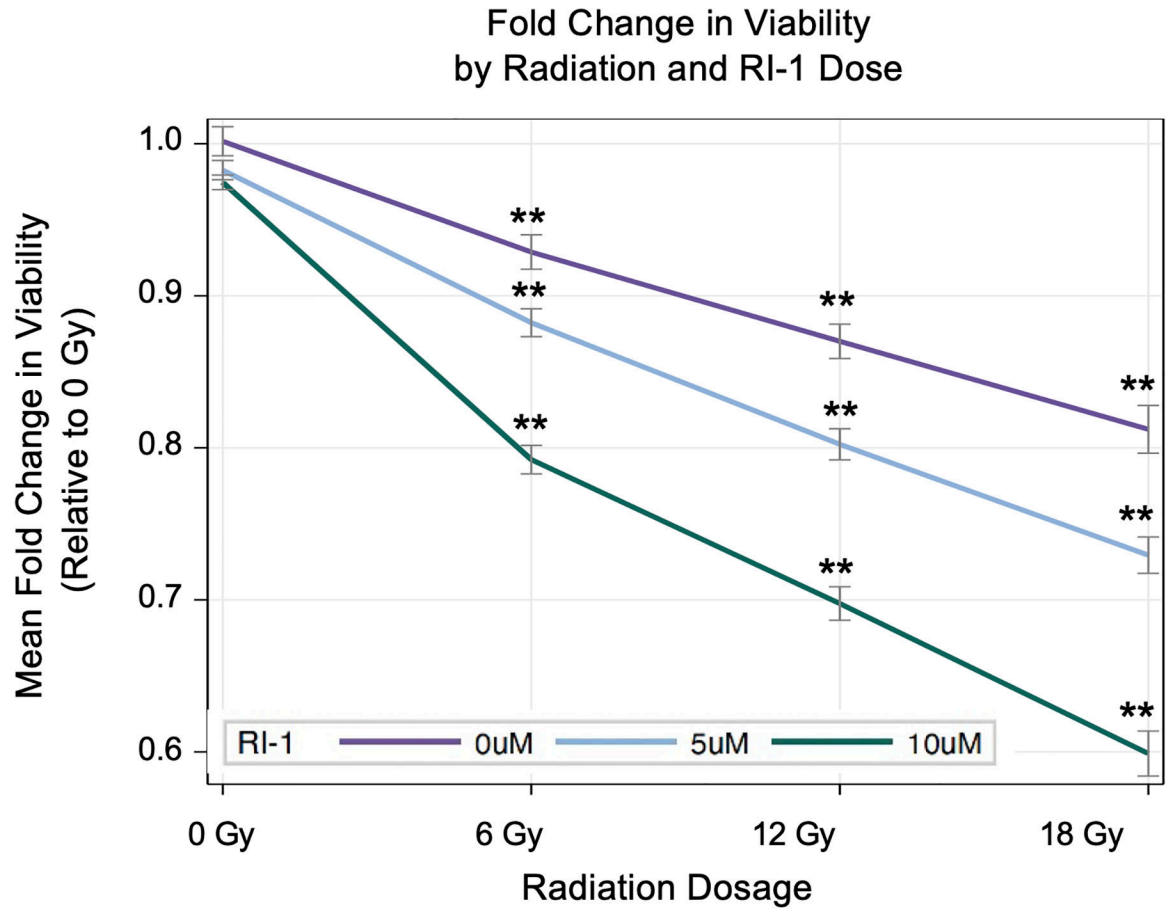


**Figure 1. Magnetic Resonance Imaging (MRI) of Vestibular Schwannoma.**

Axial T1-weighted MRI images with gadolinium for the ten vestibular schwannoma patients included in the study. Arrows point to vestibular schwannoma.



Line = Mean Fold Change at 96 hours.  
 Error bar = Standard Error Mean.  
 \*\*p<0.001

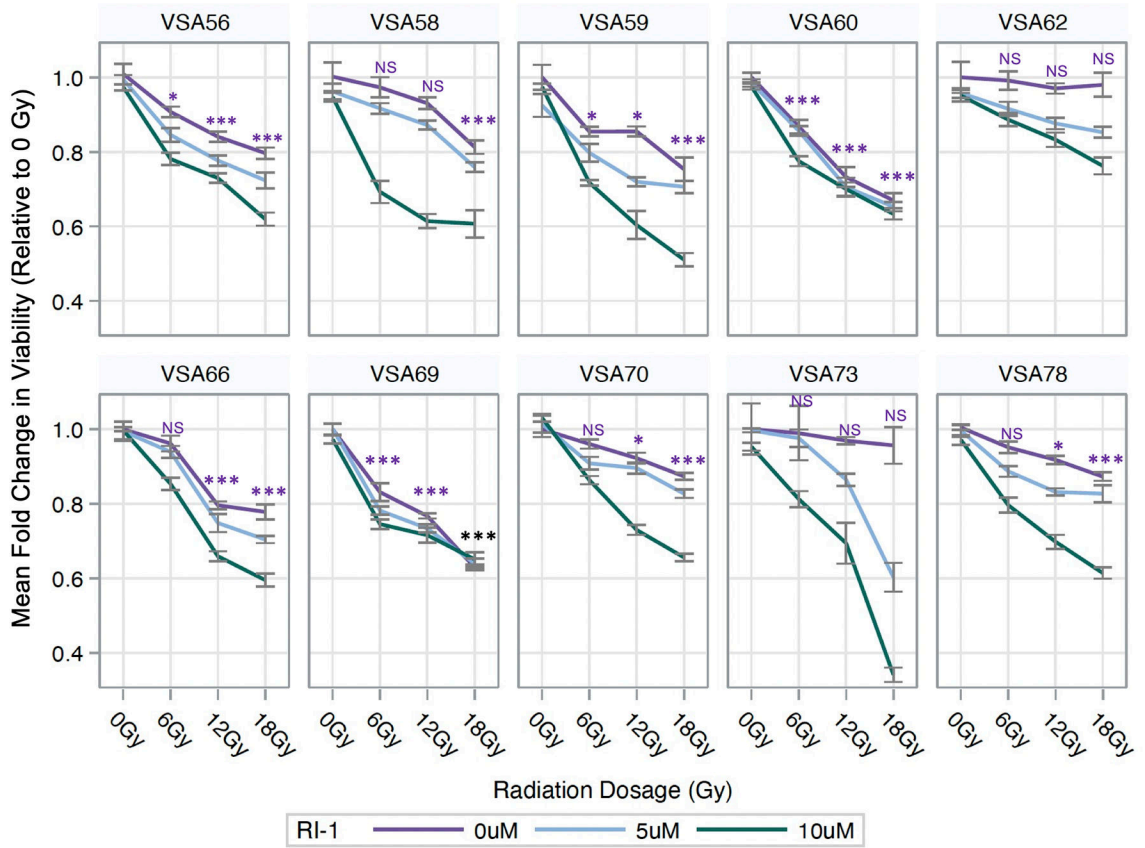
**Figure 2. Viability of Vestibular Schwannoma Cells by Radiation and RI-1 Dose.**  
 Radiation initiated dose-dependent losses in viability, when compared to 0 Gy. RI-1 treatment enhanced radiation-induced losses in viability.

Author Manuscript

Author Manuscript

Author Manuscript

Author Manuscript



Line = Mean Fold Change at 96 hours. Error Bar = Standard Error Mean.  
 For 0  $\mu$ M RI-1: \*\*\* p<0.0001, \*\* p<0.001, \* p<0.05, NS = Not Significant

**Figure 3. Viability by Tumor, Radiation, and RI-1 Dose.**

Although RI-1 (5 and 10  $\mu$ M) enhanced radiation toxicity in most tumors, RI-1 was less effective at reducing viability with VSA60 and VSA69.

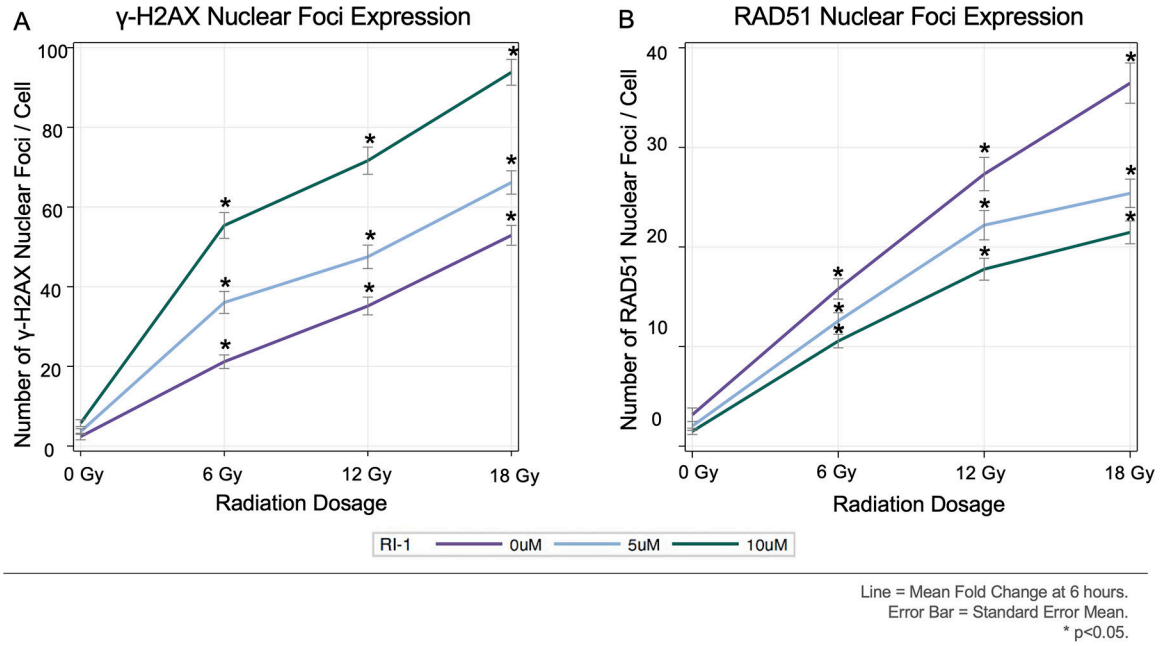


**Figure 4. Expression of  $\gamma$ -H2AX and RAD51 by Radiation and RI-1 Dose.**  
[A-B] Radiation caused dose-dependent increases in  $\gamma$ -H2AX and RAD51 nuclear foci/cell. RI-1 reduced RAD51 and increased  $\gamma$ -H2AX.

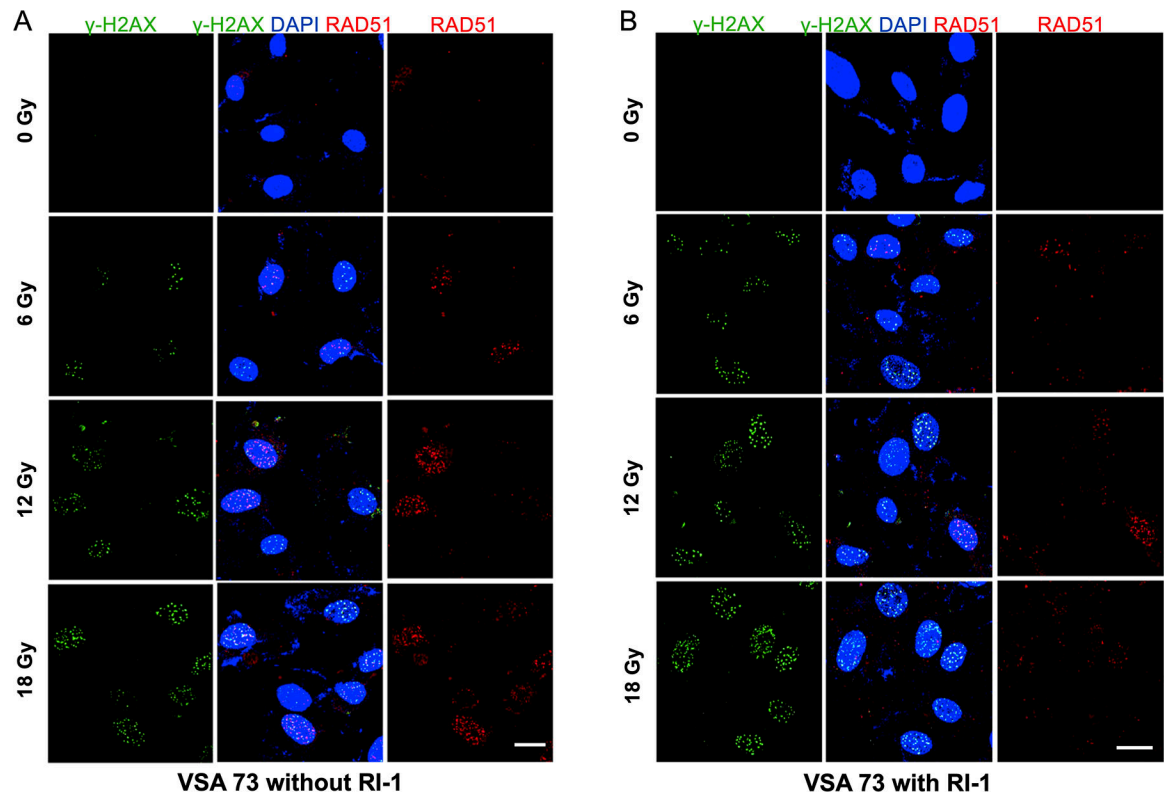
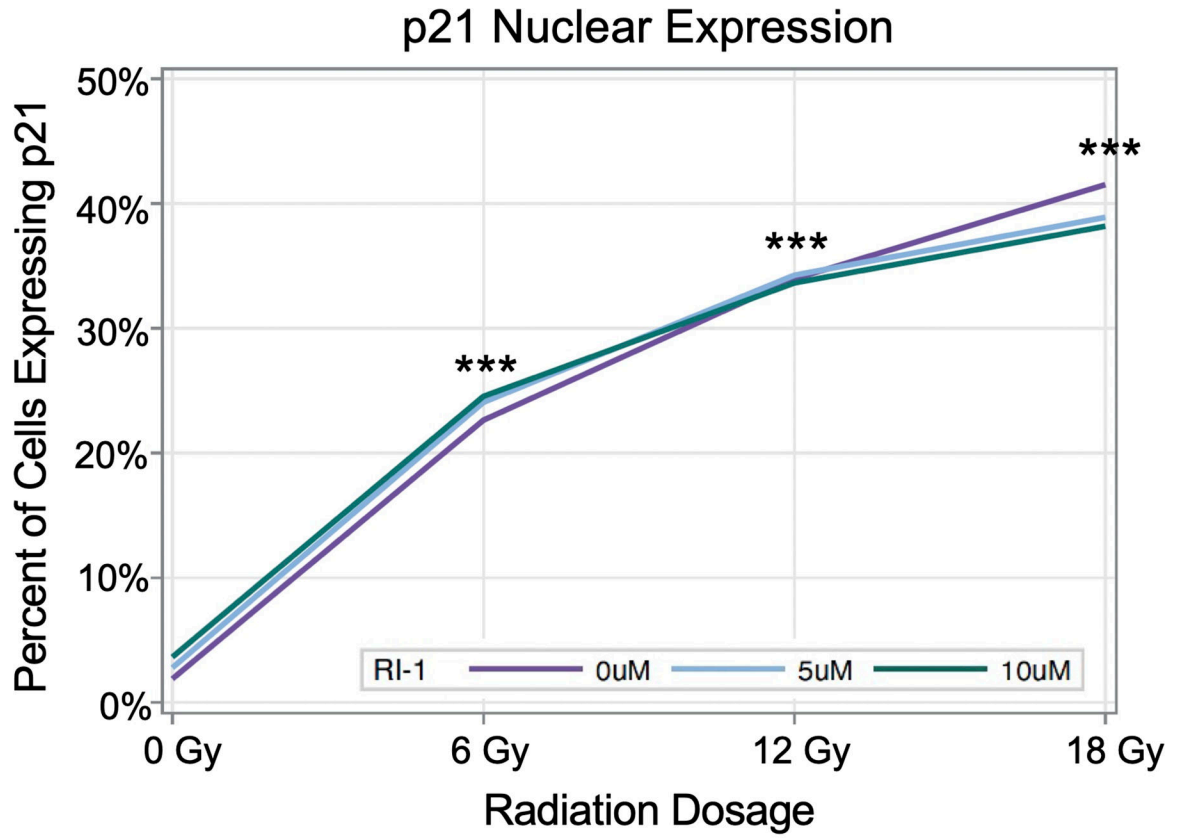


**Figure 5. Immunofluorescent Staining for  $\gamma$ -H2AX and RAD51 for VSA60.**

[A] Confocal images showing formation of  $\gamma$ -H2AX and RAD51 nuclear foci after radiation exposure. [B] RI-1 reduced RAD51 and increased  $\gamma$ -H2AX.

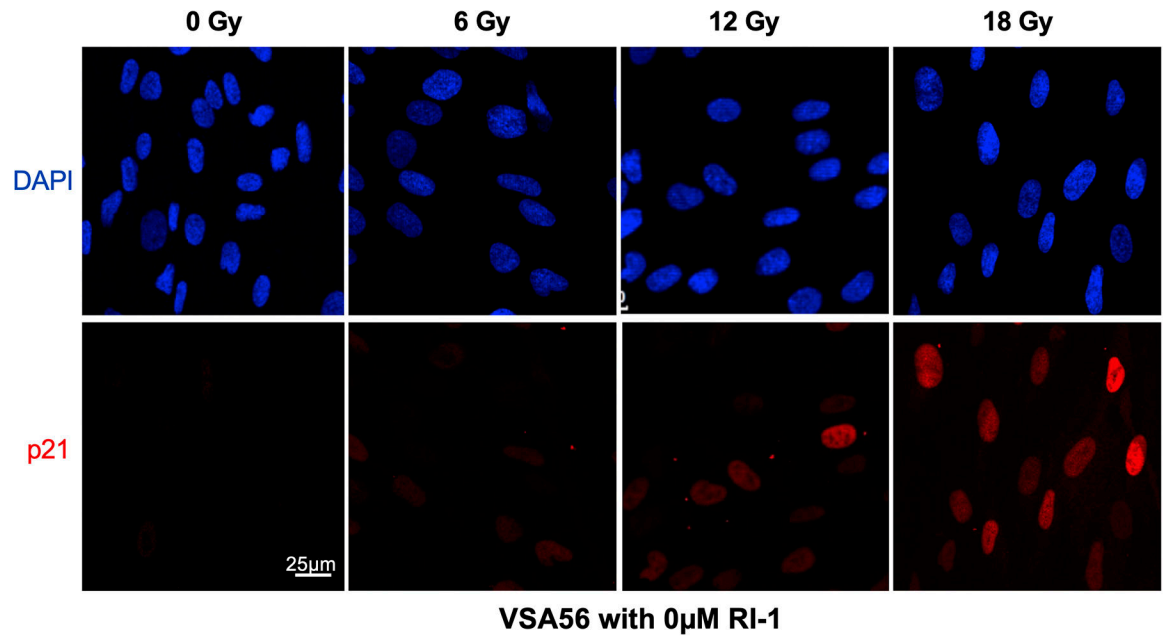


Line = Percent of Cells Expressing p21  
\*\*\* p<0.0001

**Figure 6. Nuclear p21 Expression by Radiation and RI-1 Dose.**

Radiation significantly increased the percentages of cells expressing nuclear p21 in a dose-dependent manner. No statistical difference was seen between RI-1 groups.





Representative Confocal Images (40X lens) 6 hours after irradiation.  
DAPI represents nuclear staining.

**Figure 7. Nuclear p21 expression for VSA56 at 0 μM RI-1.**

Radiation increased p21 nuclear expression in a dose-dependent manner, suggesting that higher radiation doses may initiate more cell cycle arrest.

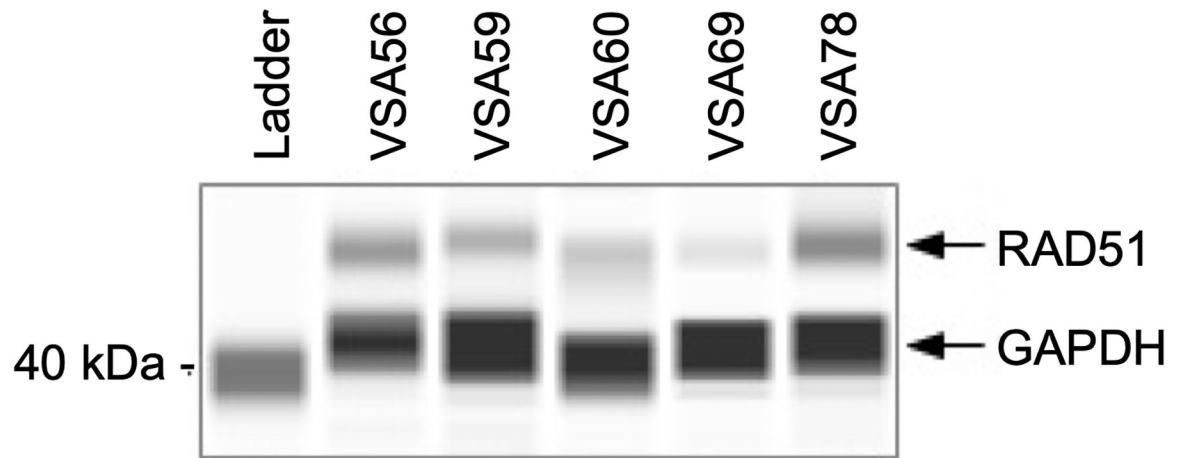


**Figure 8. Capillary Western Blotting for RAD51 Expression in Vestibular Schwannoma.** RAD51 protein was expressed in variable amounts in five tumor chunks. GAPDH was used as a housekeeping protein.

**Table 1.**

Clinical and Surgical Information for Ten Patients with Vestibular Schwannoma

Patient	Sex	Age (Years)	Tumor Volume (cm <sup>3</sup> )	Extent of Tumor Resection	SRT (dB)	WRS (%)	AAO-HNS Hearing Classification
VSA56	M	56	8.92	Near Total	NR	CNT	D
VSA58	M	30	4.53	Gross Total	95	0	D
VSA59	M	72	1.23	Gross Total	20	92	A
VSA60	F	61	0.55	Gross Total	50	24	D
VSA62	M	39	6.20	Gross Total	90	72	C
VSA66	F	72	5.96	Gross Total	NR	CNT	D
VSA69	M	31	15.25	Near Total	55	76	D
VSA70	M	47	9.87	Subtotal	25	88	A
VSA73	F	28	10.97	Near Total	45	8	D
VSA78	F	29	18.34	Subtotal	NR	CNT	D
<i>Average</i>		<b>46.5</b>	<b>8.18</b>				

Acronyms: AAO-HNSF, American Academy of Otolaryngology – Head and Neck Surgery; CNT, could not test; F, female; M, male; NR, no response; SRT, speech recognition threshold; WRS, word recognition score